In order to verify this assumption, atomic force microscopy (AFM) analysis was used to investigate the surface morphology of Si thin film before and after laser irradiation. Figure 5.12 ~ Figure 5.15 display the AFM images of the Si thin films with 1500Å- and 2000Å-thick spacer heights before and after laser irradiation, respectively. For the 1500Å-thick a-Si spacer, two apparent spacers with 1500Å-height are observed before laser irradiation. After laser crystallization, however, the spacers disappear at the film surface. This means that the most of the a-Si at the spacer region are molten after laser irradiation for the 1500Å-thick case. On the other hand, for the poly-Si thin film with 2000Å-thick a-Si spacer, the spaces still exist after laser irradiation. This represents that the laser fluence is only sufficient to melt part of the a-Si spacer in depth, which is consistence with the SEM results.

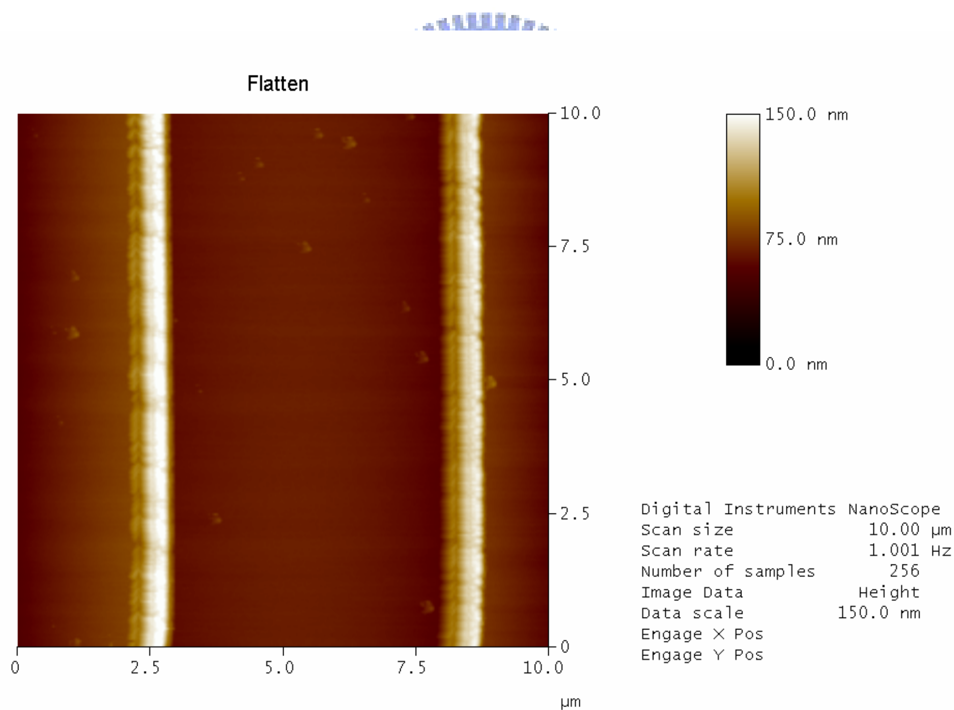

(a)

Figure 5.12. AFM images of the Si thin film with 1500Å-thick spacer heights before laser irradiation (a) flat image (b) 3-D image

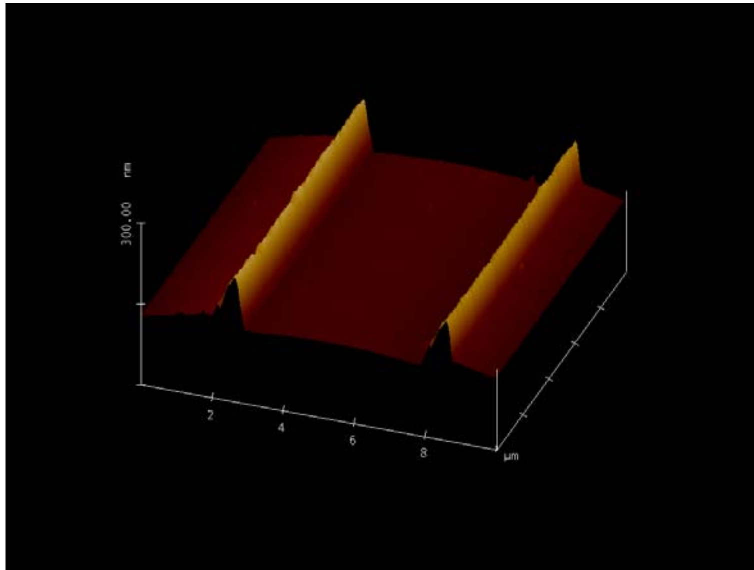

(b)

Figure 5.12. AFM images of the Si thin film with 1500Å-thick spacer heights before laser irradiation (a) flat image (b) 3-D image.

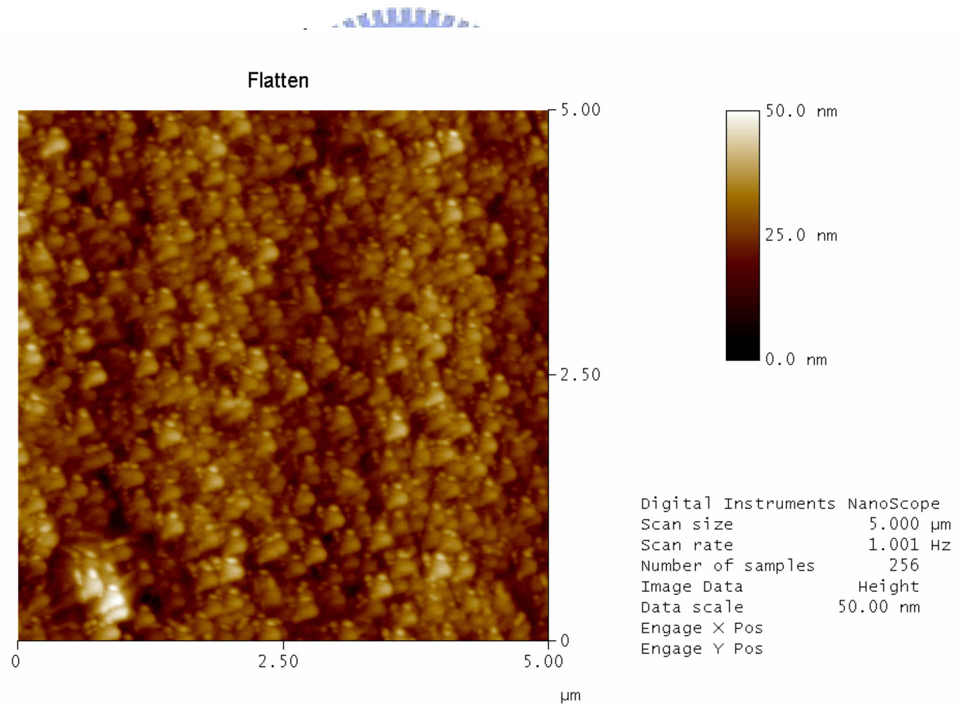

(a)

Figure 5.13. AFM images of the Si thin film with 1500Å-thick spacer heights after laser irradiation (a) flat image (b) 3-D image.

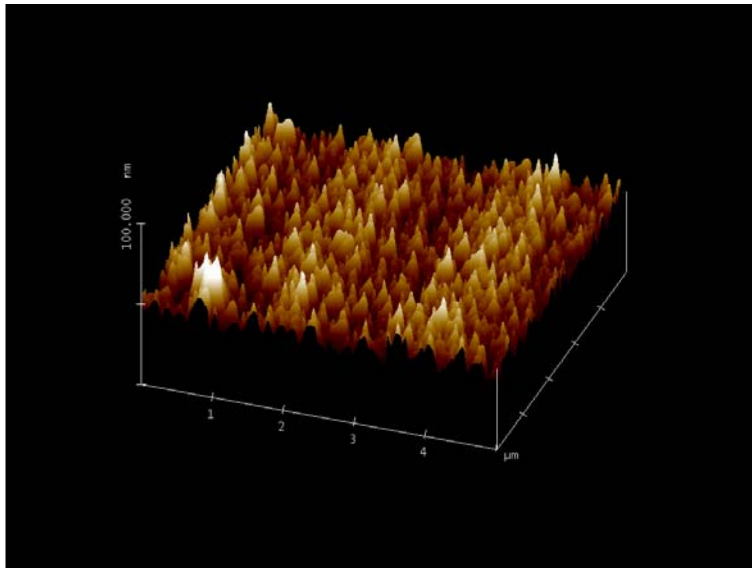

(b)

Figure 5.13. AFM images of the Si thin film with 1500Å-thick spacer heights after laser irradiation (a) flat image (b) 3-D image.

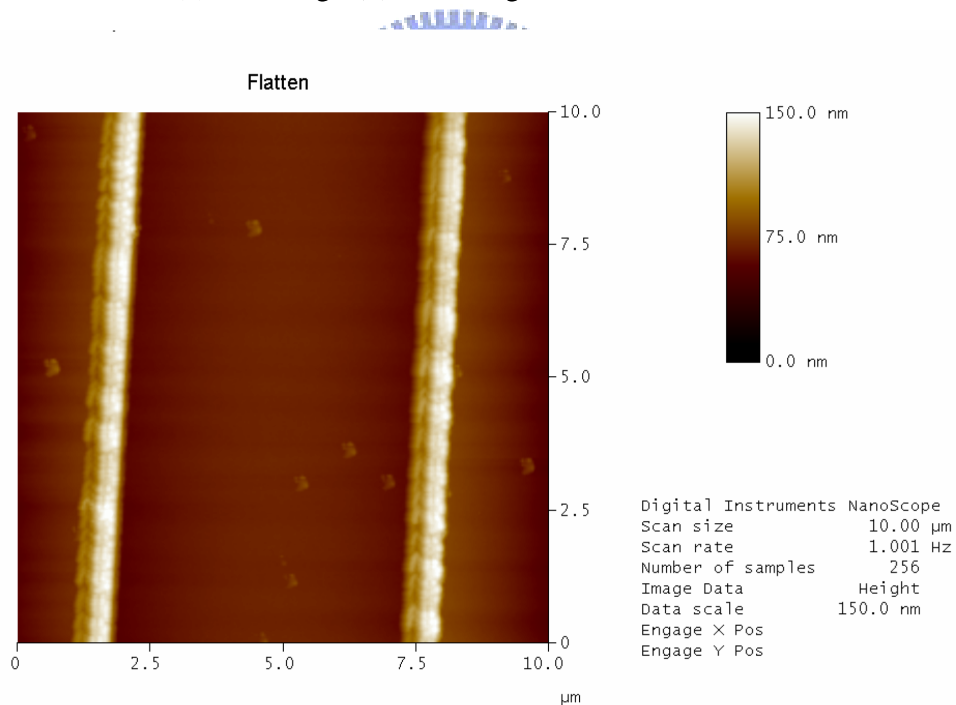

(a)

Figure 5.14. AFM images of the Si thin film with 2000Å-thick spacer heights before laser irradiation (a) flat image (b) 3-D image.

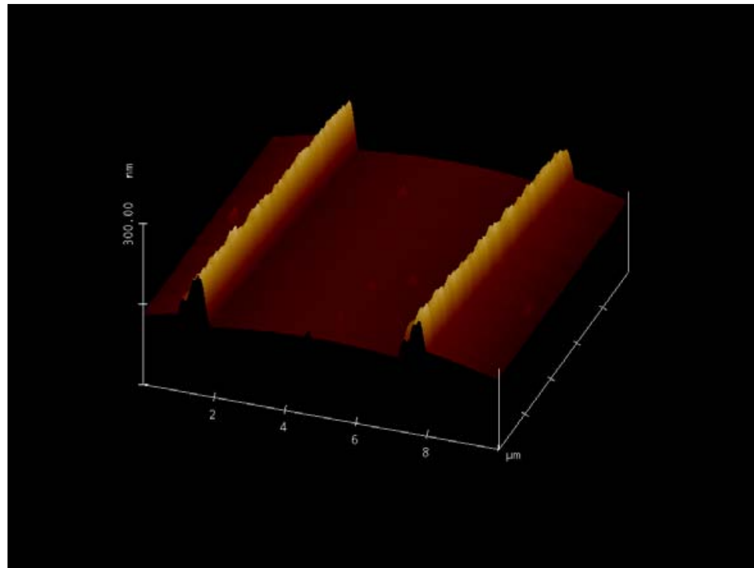

(b)

Figure 5.14. AFM images of the Si thin film with 2000Å-thick spacer heights before laser irradiation (a) flat image (b) 3-D image.

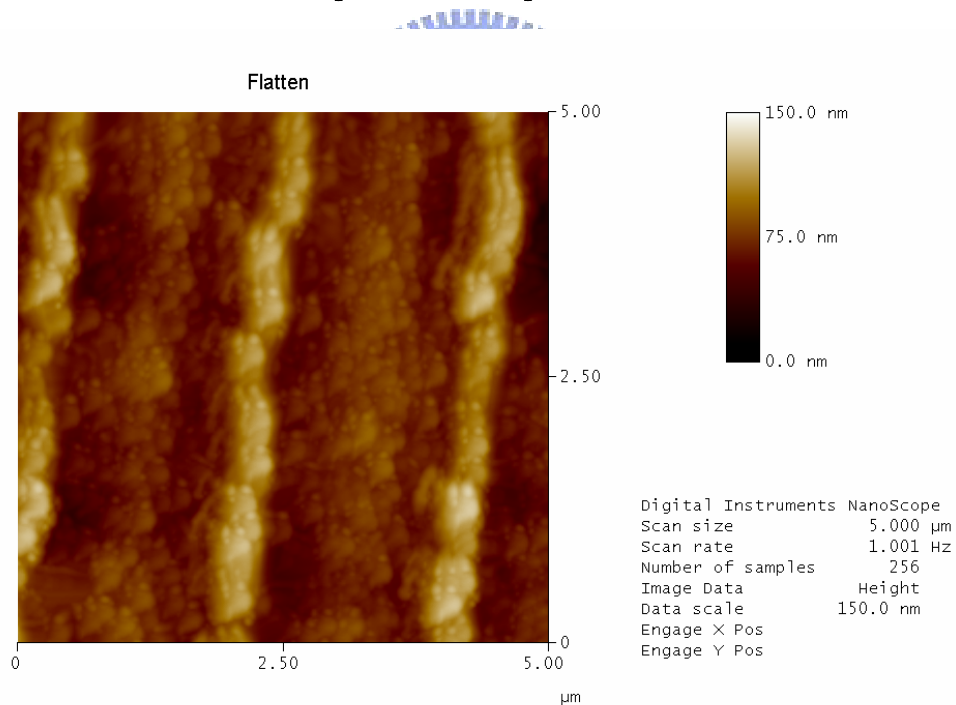

(a)

Figure 5.15. AFM images of the Si thin film with 2000Å-thick spacer heights after laser irradiation (a) flat image (b) 3-D image.

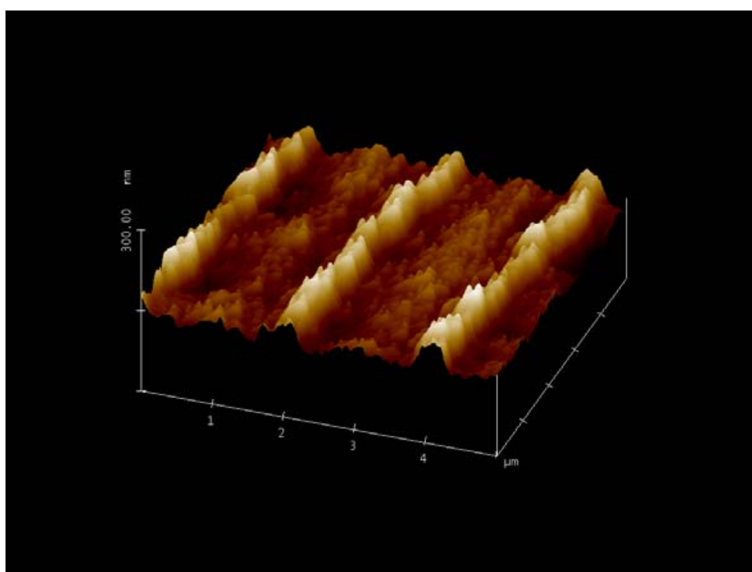

(b)

Figure 5.15. AFM images of the Si thin film with 2000Å-thick spacer heights after laser irradiation (a) flat image (b) 3-D image.

The crystallization mechanism of the poly-Si thin film with 2000Å-thick a-Si spacer is illustrated in Figure 5.16. When laser irradiation is performed, only parts of the a-Si at the spacer region can be melted and there are still large amounts of retained solid a-Si nucleation seeds remaining at the spacer region. An apparent vertical temperature gradient will exist at the spacer region, which results in a grain growth behavior obeying the regrowth mechanism in the partial-melting regime. As the solidification process progresses, grain growth starts vertically to the film surface as well as horizontally to the adjacent region from the nucleation seed. Thus, for the poly-Si thin films with 2000Å-thick a-Si spacers, many small grains are found at the spacer region accompanying with longitudinal grains next to them. These small grains will have a profound influence on the performance of poly-Si TFTs crystallized with 2000Å-thick a-Si spacer structure, which will be discussed in the next section.

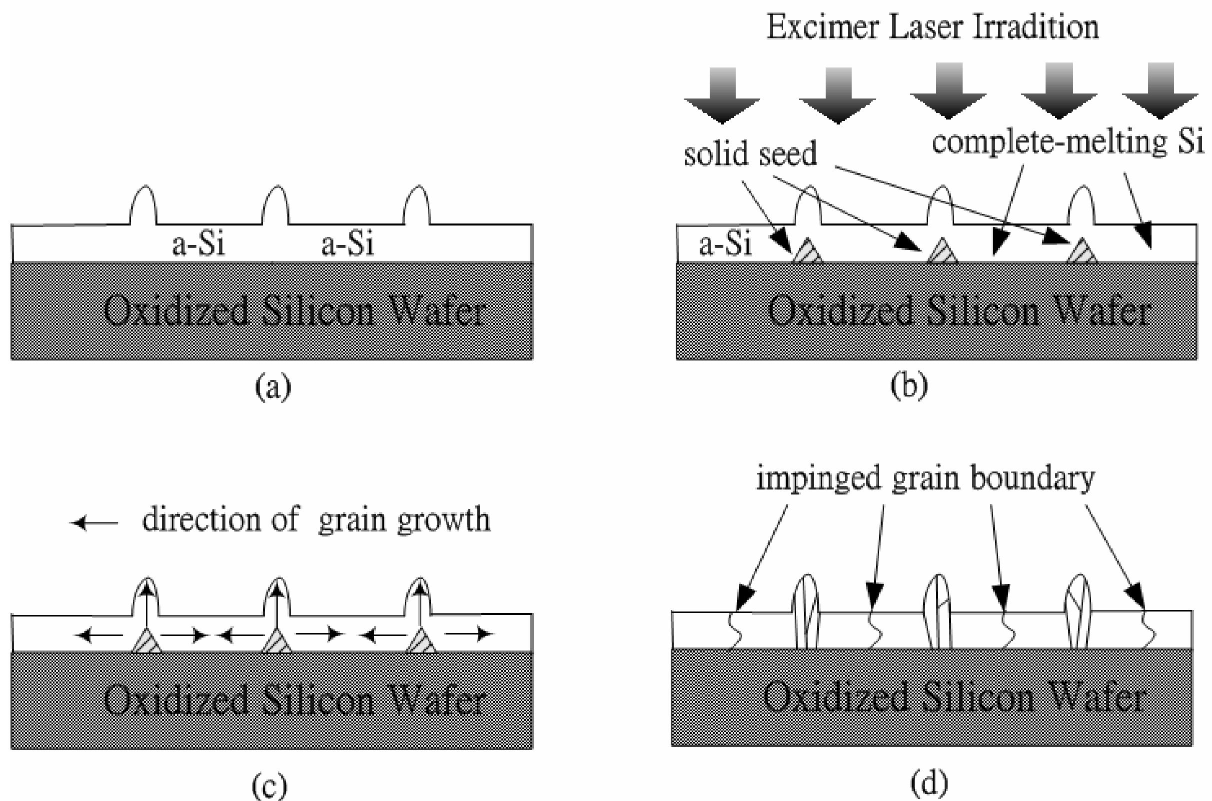

Figure 5.16. The crystallization mechanism of the poly-Si thin film with 2000Å-thick a-Si spacer.

5.4.2 Electrical Characteristics of Small Dimension Poly-Si Thin Film Transistors with a-Si Spacer Structure

5.4.2.1 a-Si Spacer with a Thickness of 1500Å

In the previous section, it has been demonstrated that large and longitudinal grains can be produced in the channel by adopting a-Si spacer structure. The grain structure will have a profound influence on the electrical characteristics of the fabricated TFTs. Figure 5.17(a) ~ Figure 5.17(e) show the typical transfer characteristics of poly-Si TFTs crystallized using a-Si spacer structure with channel lengths of 1.5 μm ~ 5 μm, in which the thickness of a-Si spacer

is 1500Å. The laser process conditions are optimized. The conventional TFTs are also shown for comparison. Several important electrical characteristics of the TFTs are summarized in Table 5.1. The threshold voltage is defined as the gate voltage required to achieve a normalized drain current of I_d = - (W/L) x 10^{-8} A at $|V_{ds}|$ = 0.1V. The field effect mobility is extracted from the maximum transconductance in the linear region of I_d-V_g characteristics at $|V_d|$ = 0.1V. The on/off current ratio is specified by the maximum drain current at $|V_{ds}|$ = 5V and $|V_{gs}|$ = 20V over the minimum drain current at $|V_{ds}|$ = 5V.

Table 5.1. Measured optimal electrical characteristics of TFTs crystallized with a-Si spacer and conventional structure. The a-Si spacer thickness is 1500Å.

W / L (μm/μm)	Structure	Threshold Voltage (V)	Mobility (cm^2/V-s)	Subthreshold Swing (mV/dec)	I_{on}/I_{off} @ V_{ds} = -5V
1.5 μm	conventional	-0.65	154	1072	$1.68x10^6$
	a-Si spacer	-0.44	302	807	$8.68x10^7$
2 μm	conventional	1.94	128	737	$3.32x10^7$
	a-Si spacer	0.98	288	672	$3.68x10^7$
3 μm	conventional	3.72	115	1010	$3.41x10^7$
	a-Si spacer	3.53	205	943	$6.81x10^7$
4 μm	conventional	3.44	107	778	$6.23x10^6$
	a-Si spacer	2.29	197	703	$5.73x10^7$
5 μm	conventional	4.99	96	1170	$1.04x10^7$
	a-Si spacer	4.84	169	1170	$3.6x10^7$

According to these figures, the poly-Si TFTs with a-Si spacer structure exhibit better electrical characteristics than conventional ones. This can be attributed to the longitudinal grain in the device channel region. Take the dimension of W = L = 2 μm for example, poly-Si TFT with field effect mobility of about 288 cm^2/V-s can be achieved by using this a-Si spacer method while the mobility of the conventional counterpart is about 128 cm^2/V-s. In addition, although the maximum achievable length of lateral grain growth is limited between 2 μm to 2.5 μm as described in the previous section, the electrical characteristics of the TFTs with device dimension up to W = L = 5 μm are still superior to those of conventional ones. This can also ascribed to the long longitudinal grain growth even though many small grains resulted from spontaneous nucleation exist in the channel region as well.

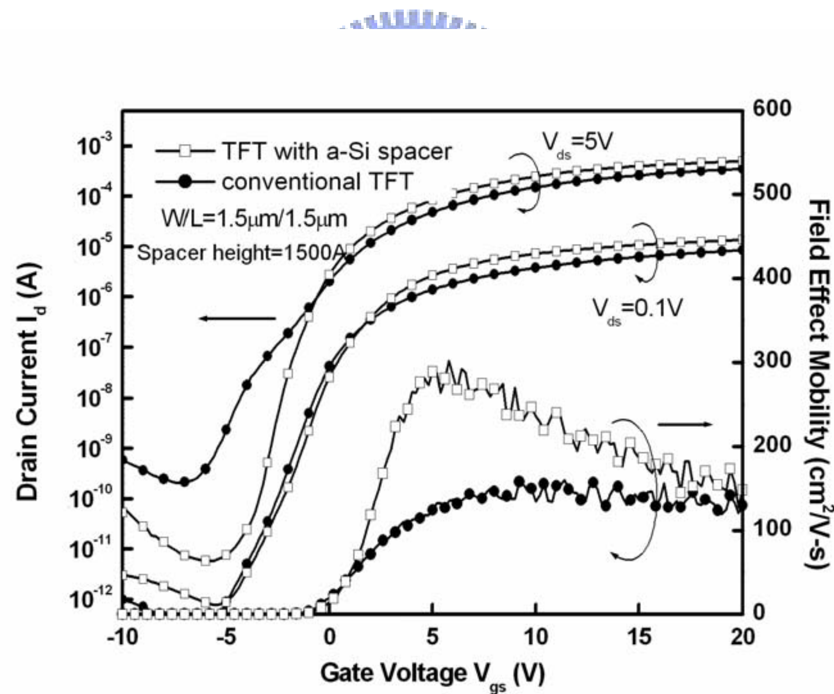

Figure 5.17(a). The typical transfer characteristic of poly-Si TFTs crystallized using a-Si spacer structure with channel length of 1.5 μm, in which the thickness of a-Si spacer is 1500Å.

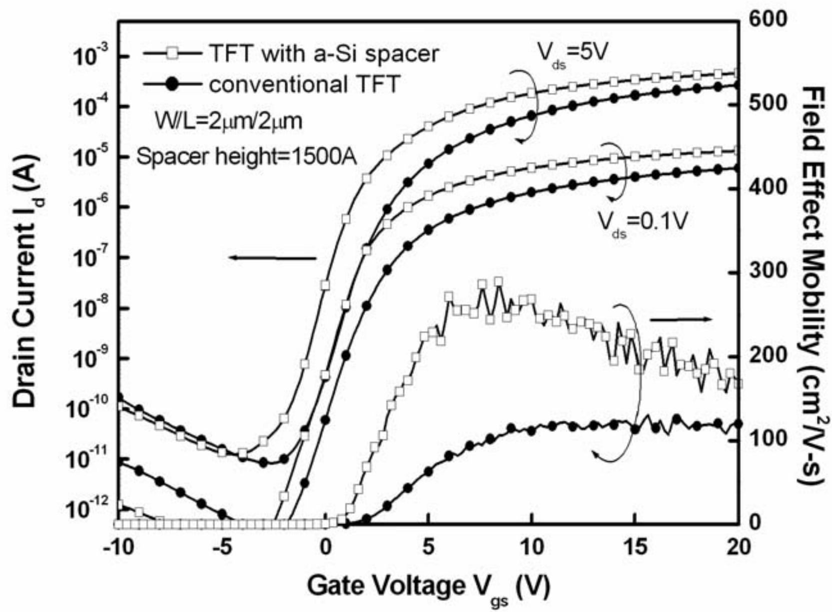

Figure 5.17(b). The typical transfer characteristic of poly-Si TFTs crystallized using a-Si spacer structure with channel length of 2 μm, in which the thickness of a-Si spacer is 1500Å.

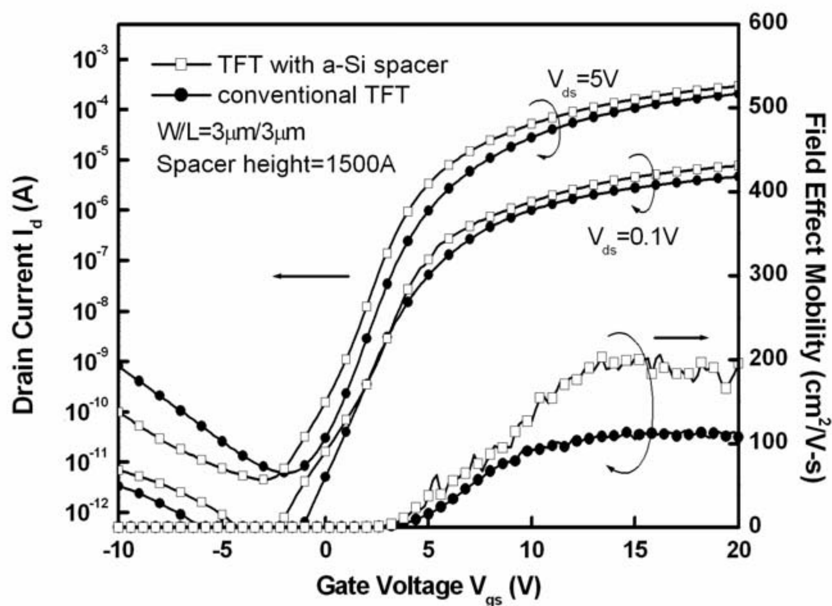

Figure 5.17(c). The typical transfer characteristic of poly-Si TFTs crystallized using a-Si spacer structure with channel length of 3 μm, in which the thickness of a-Si spacer is 1500Å.

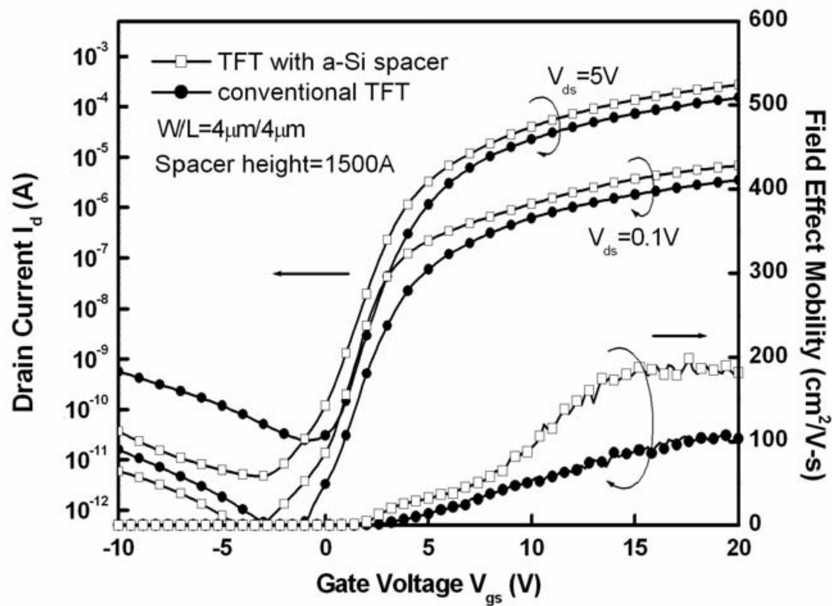

Figure 5.17(d). The typical transfer characteristic of poly-Si TFTs crystallized using a-Si spacer structure with channel length of 4 μm, in which the thickness of a-Si spacer is 1500Å.

ES A

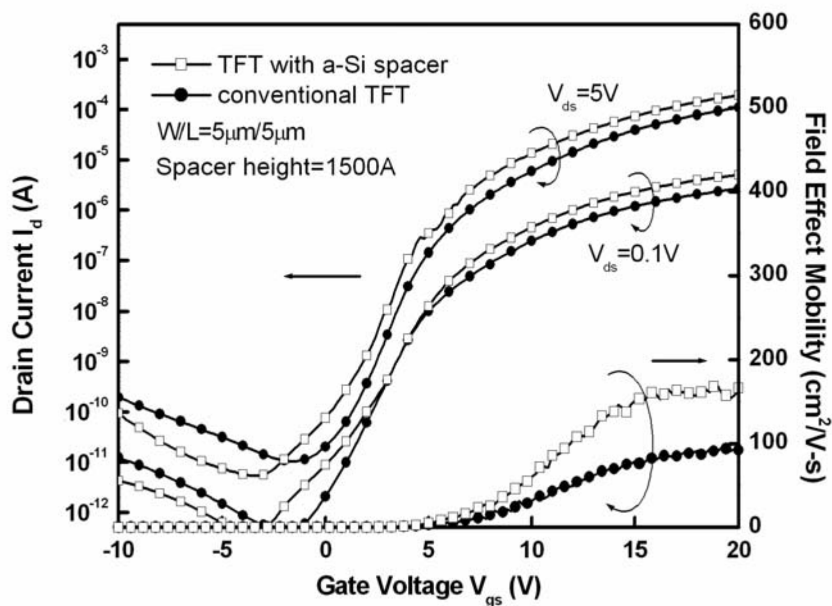

Figure 5.17(e). The typical transfer characteristic of poly-Si TFTs crystallized using a-Si spacer structure with channel length of 5 μm, in which the thickness of a-Si spacer is 1500Å.

Figure 5.18(a) ~ Figure 5.18(e) display the output characteristics poly-Si TFTs crystallized using a-Si spacer structure with channel lengths of 1.5 μm ~ 5 μm, in which the thickness of a-Si spacer is 1500Å. It is demonstrated that poly-Si TFTs with a-Si spacer structure provide higher driving current than conventional ELC poly-Si TFTs under the same bias condition. The improved driving current can be attributed to the high field effect mobility. In addition, for the TFTs device with W = L = 1.5 μm, as the applied voltage is high enough, the lack of saturation in drain current resulted from mobility degradation becomes more serious. The mobility degradation is attributed to the self-heating effect [5.57] – [5.58]. It is indicated that as the performance of poly-Si TFTs approaches to that of silicon-on-insulator (SOI) MOSFETs, power dissipation in the devices is increased, and therefore, self-heating effects become serious because of small thermal conductance of the insulating substrate. Furthermore, self-heating become more significant as the channel length is reduced since the drain current increases. Thus, the self-heating effect may be a problem for small-dimension poly-Si TFTs.

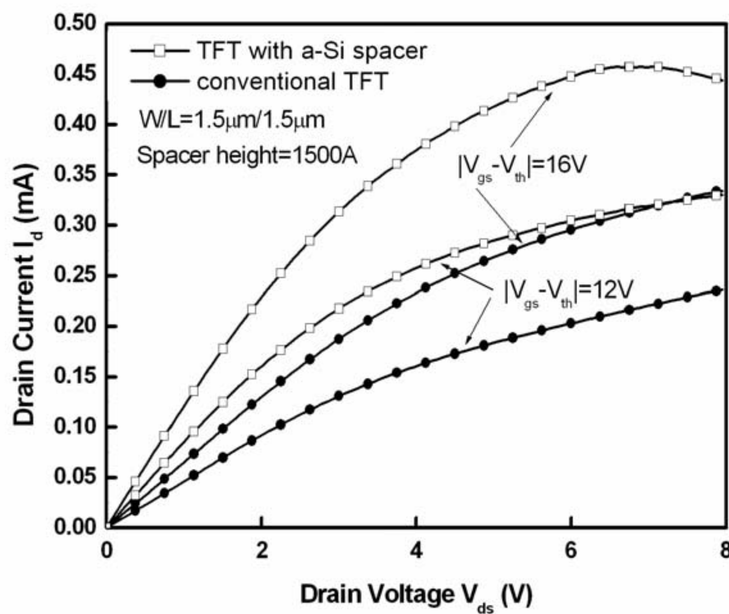

Figure 5.18(a). The output characteristic of poly-Si TFTs crystallized using a-Si spacer structure with channel length of 1.5 μm. The a-Si spacer thickness is 1500Å.

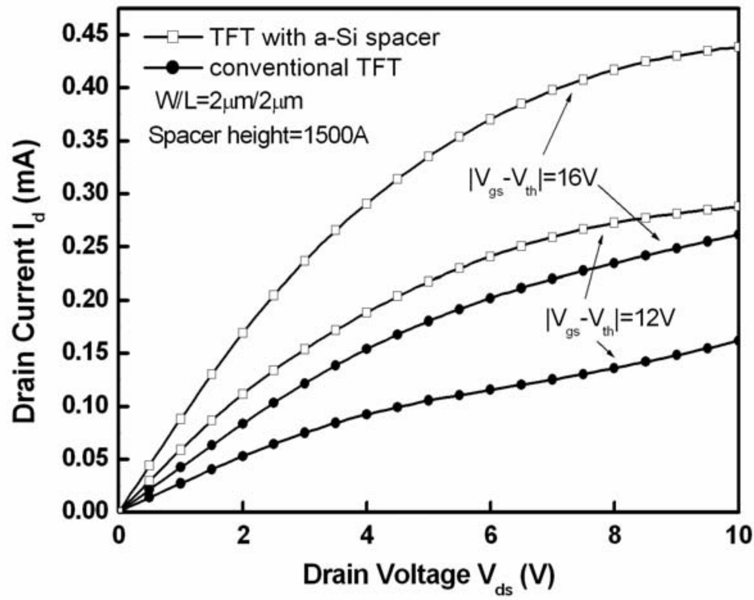

Figure 5.18(b). The output characteristic of poly-Si TFTs crystallized using a-Si spacer structure with channel length of 2 μm. The a-Si spacer thickness is 1500Å.

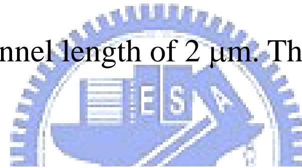

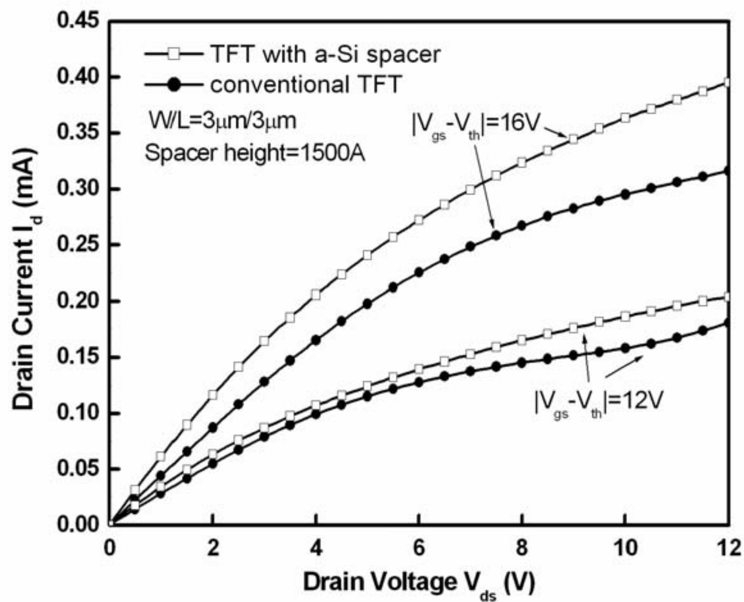

Figure 5.18(c). The output characteristic of poly-Si TFTs crystallized using a-Si spacer structure with channel length of 3 μm. The a-Si spacer thickness is 1500Å.

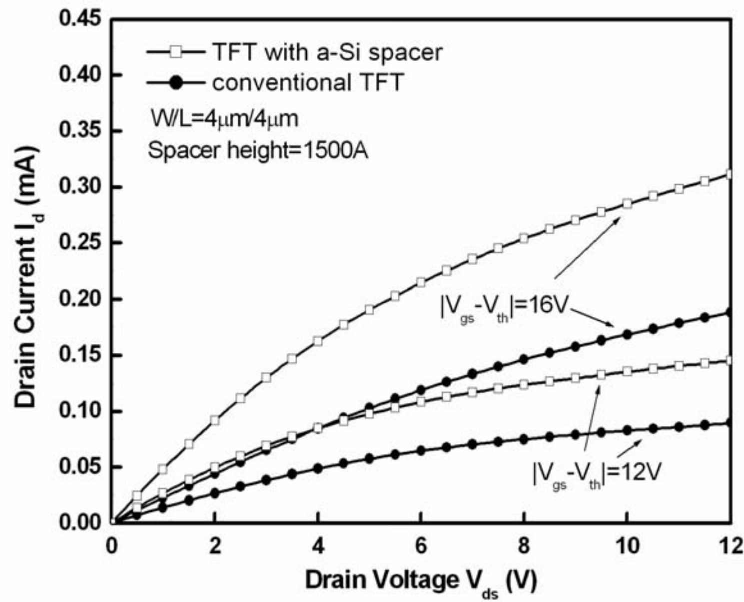

Figure 5.18(d). The output characteristic of poly-Si TFTs crystallized using a-Si spacer structure with channel length of 4 μm. The a-Si spacer thickness is 1500Å.

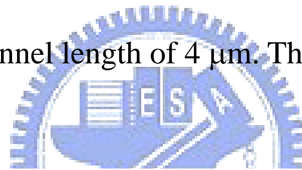

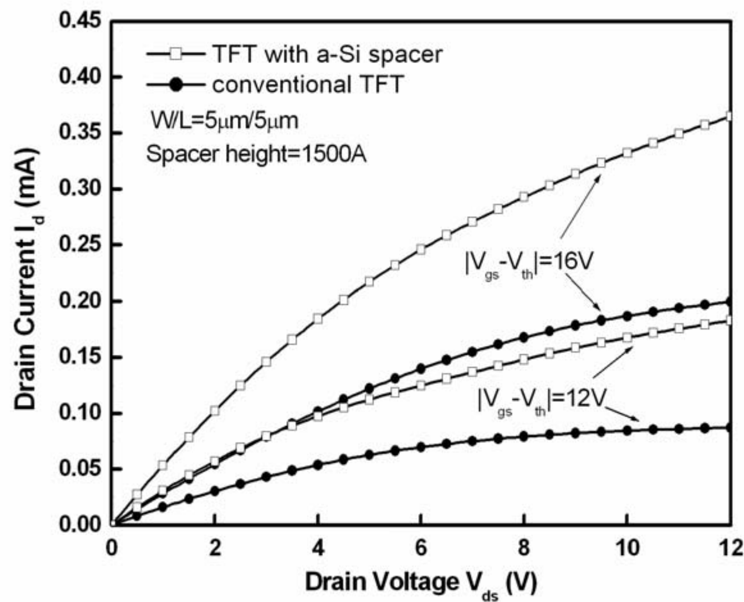

Figure 5.18(e). The output characteristic of poly-Si TFTs crystallized using a-Si spacer structure with channel length of 5 μm. The a-Si spacer thickness is 1500Å.

In addition to the enhancement of poly-Si TFT performance, poly-Si TFT crystallized with a-Si spacer structure also exhibited better uniformity due to the wide laser process window. Figure 5.19 shows the dependence of field-effect mobility on the applied laser energy density for poly-Si TFTs crystallized with two different structures. The channel length and width are both 2μm. Twenty TFTs are measured for each laser irradiation condition to investigate the device-to-device variation. The vertical bars in the figures indicate the minimum and maximum characteristic values found at the specific laser energy density, and the solid symbols are the average calculated characteristic values. Compared to the conventional poly-Si TFT, it can be found that for the poly-Si TFT with a-Si spacer structure, the field-effect mobility is much less sensitive to the variation of laser energy density and good uniformity of field-effect mobility is obtained as the applied laser energy density exceeds beyond a certain threshold value. This yields that a wide laser process window is obtained in this crystallization method.

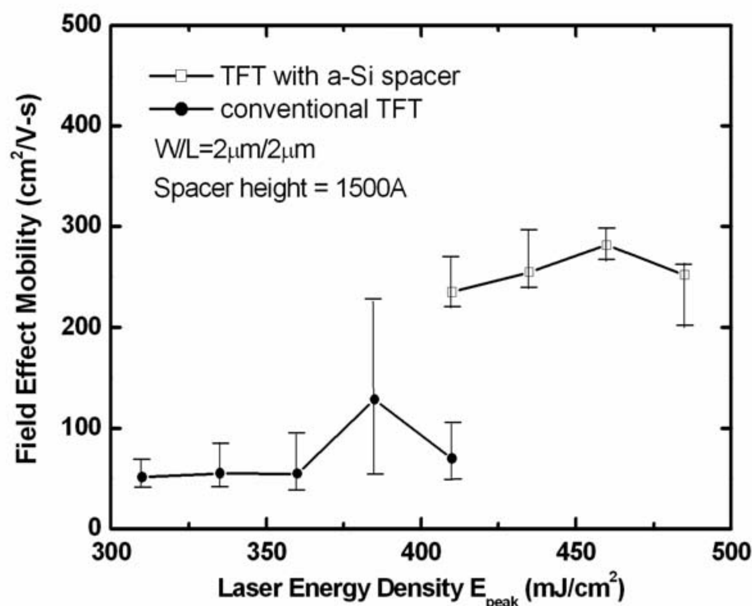

Figure 5.19. The dependence of field-effect mobility on the applied laser energy density for poly-Si TFTs crystallized with a-Si spacer and conventional structures.

5.4.2.2 a-Si Spacer with a Thickness of 2000Å

Figure 5.20(a) ~ Figure 5.20(e) show the typical transfer characteristics of poly-Si TFTs crystallized using a-Si spacer structure with channel lengths of 1.5 μm ~ 5 μm, in which the thickness of a-Si spacer is 2000Å. The laser process conditions are optimized. Several important electrical characteristics of the TFTs are summarized in Table 5.2. Although fine and small grains are observed at the 2000Å-thick spacer region as discussed in the previous section, the poly-Si TFTs with a 2000Å-thick a-Si spacer still exhibit high field effect mobility than those of conventional counterparts. The high mobility is also attributed to the longitudinal grains in the channel region. Under 2 μm design rule, the poly-Si TFT with field effect mobility of about 265 cm^2/V-s can be achieved by using this a-Si spacer method while the mobility of the conventional one is about 128 cm^2/V-s.

Table 5.2. Measured optimal electrical characteristics of TFTs crystallized with a-Si spacer and conventional structure. The a-Si spacer thickness is 2000Å.

W / L (μm/μm)	Structure	Threshold Voltage (V)	Mobility (cm^2/V-s)	Subthreshold Swing (mV/dec)	I_{on}/I_{off} @ V_{ds} = -5V
1.5 μm	conventional	-0.65	154	1072	$1.68x10^6$
	a-Si spacer	-0.25	257	546	$2.25x10^7$
2 μm	conventional	1.94	128	737	$3.32x10^7$
	a-Si spacer	-0.05	265	712	$5.59x10^7$
3 μm	conventional	3.72	115	1010	$3.41x10^7$
	a-Si spacer	0.79	188	786	$1.20x10^7$
4 μm	conventional	3.44	107	778	$6.23x10^6$
	a-Si spacer	2.53	173	1247	$5.86x10^6$
5 μm	conventional	4.99	96	1170	$1.04x10^7$
	a-Si spacer	4.10	170	1442	$9.48x10^6$

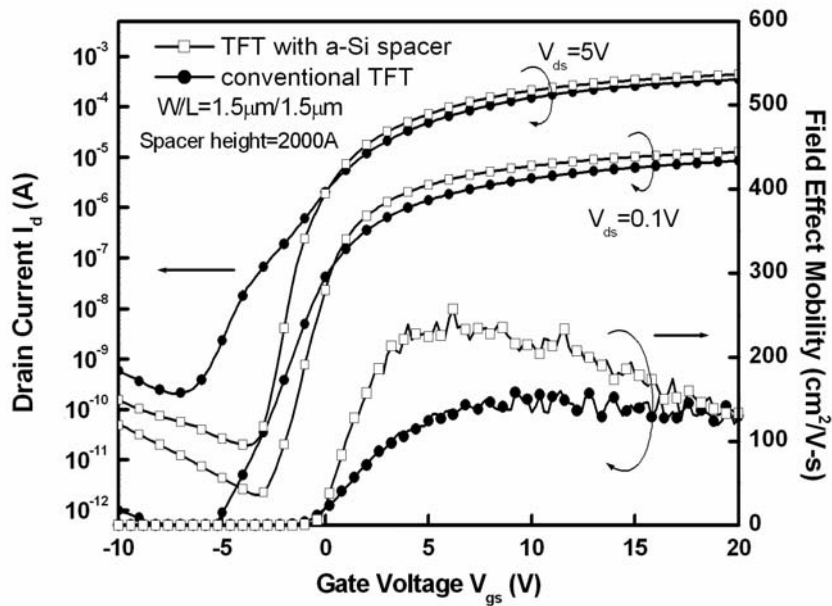

Figure 5.20(a). The typical transfer characteristic of poly-Si TFTs crystallized using a-Si spacer structure with channel length of 1.5 μm, in which the thickness of a-Si spacer is 2000Å.

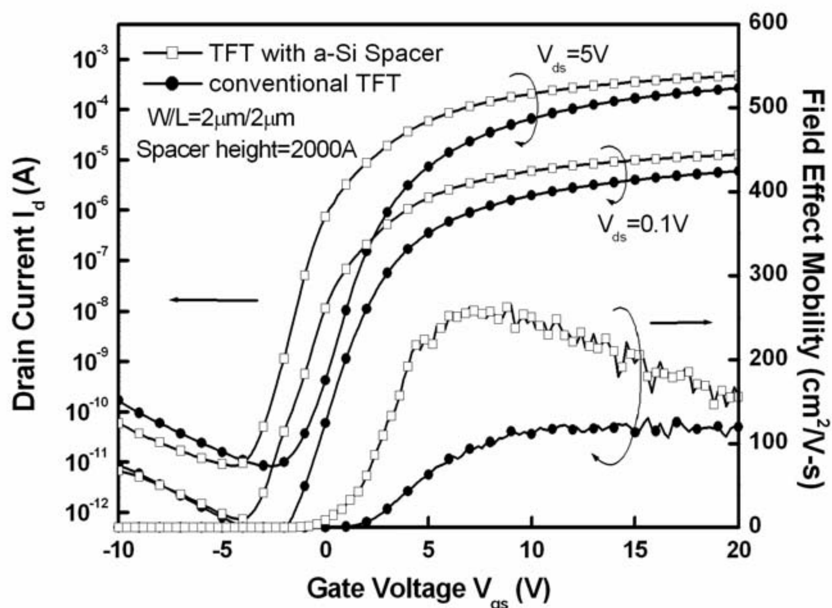

Figure 5.20(b). The typical transfer characteristic of poly-Si TFTs crystallized using a-Si spacer structure with channel length of 2 μm, in which the thickness of a-Si spacer is 2000Å.

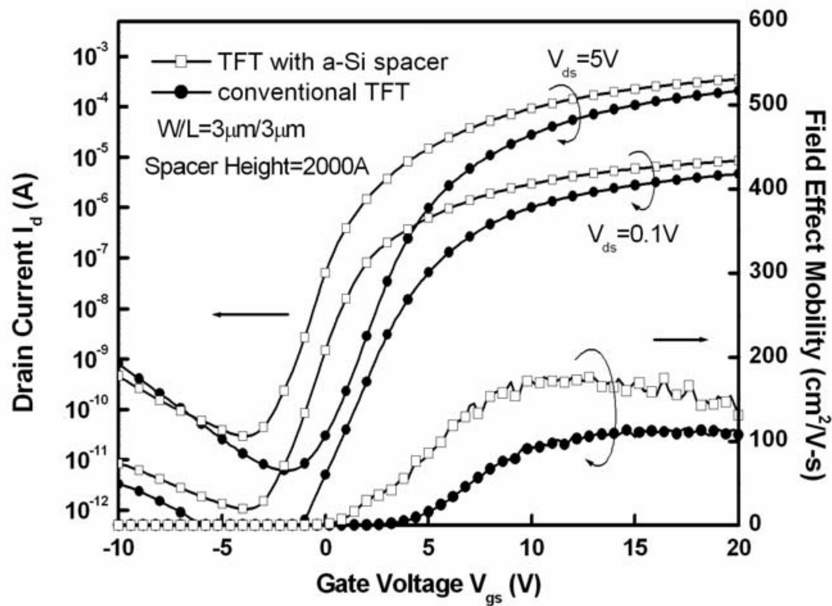

Figure 5.20(c). The typical transfer characteristic of poly-Si TFTs crystallized using a-Si spacer structure with channel length of 3 μm, in which the thickness of a-Si spacer is 2000Å.

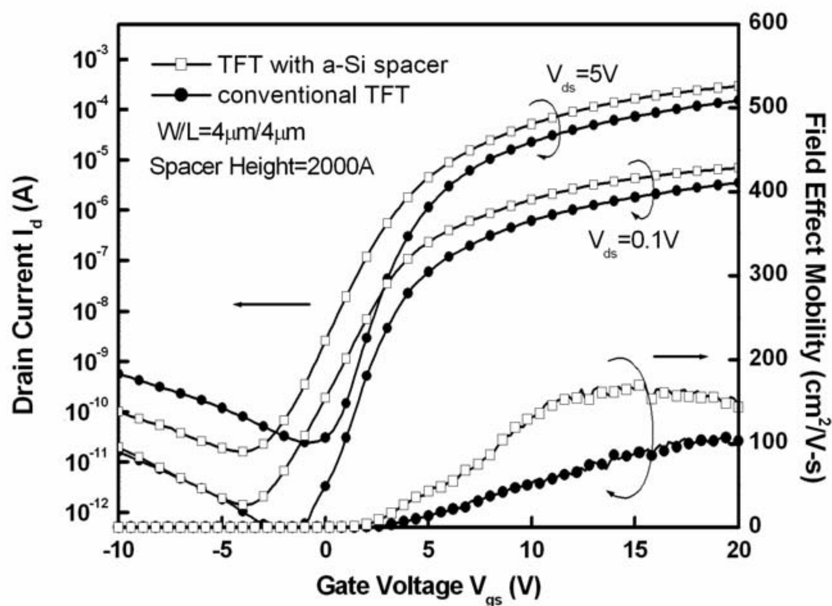

Figure 5.20(d). The typical transfer characteristic of poly-Si TFTs crystallized using a-Si spacer structure with channel length of 4 μm, in which the thickness of a-Si spacer is 2000Å.

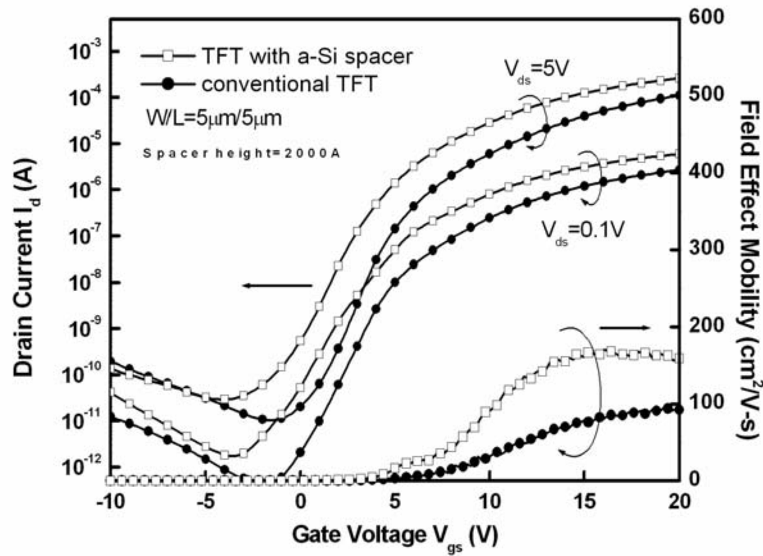

Figure 5.20(e). The typical transfer characteristic of poly-Si TFTs crystallized using a-Si spacer structure with channel length of 5 μm, in which the thickness of a-Si spacer is 2000Å.

Figure 5.21(a) ~ Figure 5.21(e) display the output characteristics of poly-Si TFTs crystallized with 2000Å-thick a-Si spacer structure. Similarly, high driving current were found in these devices due to the high field effect mobility.

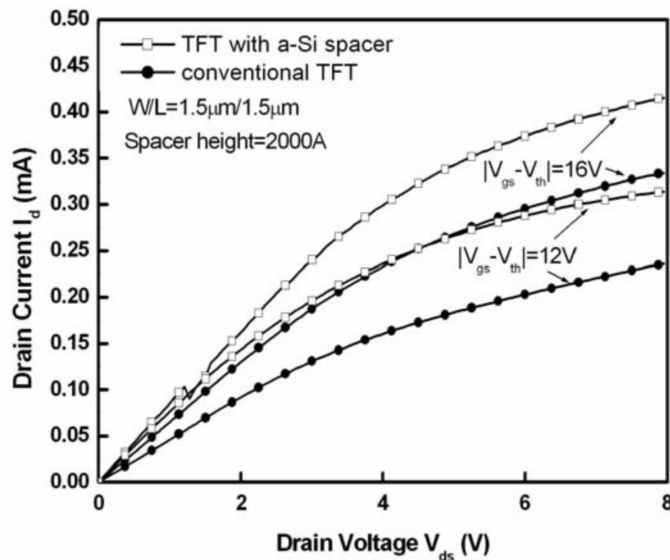

Figure 5.21(a). The output characteristic of poly-Si TFTs crystallized using a-Si spacer structure with channel length of 1.5 μm. The a-Si spacer thickness is 2000Å.

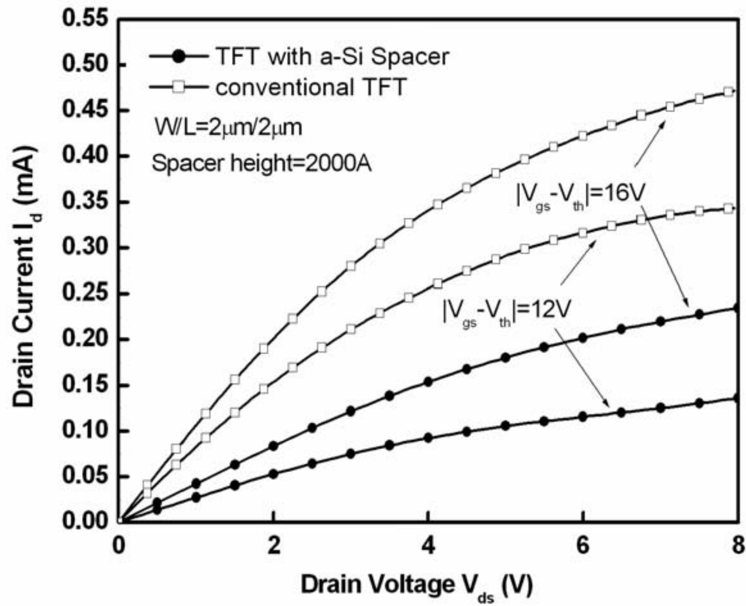

Figure 5.21(b). The output characteristic of poly-Si TFTs crystallized using a-Si spacer structure with channel length of 2 μm. The a-Si spacer thickness is 2000Å.

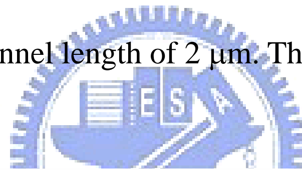

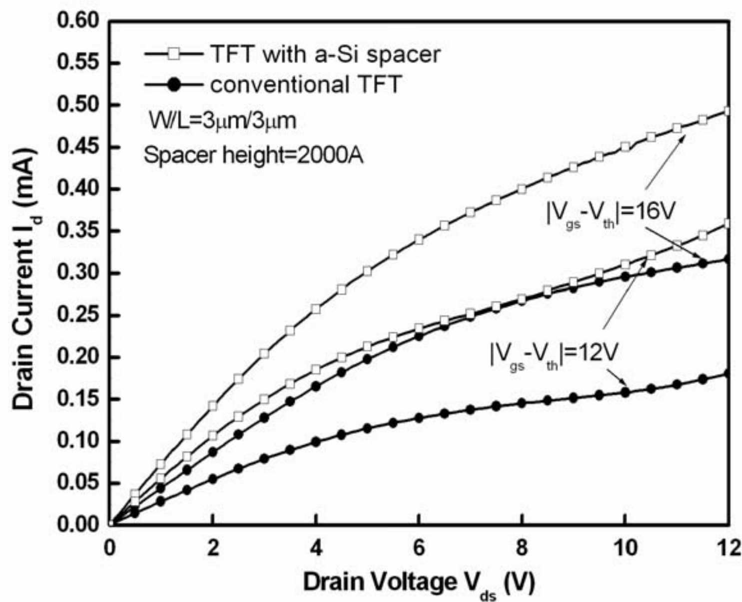

Figure 5.21(c). The output characteristic of poly-Si TFTs crystallized using a-Si spacer structure with channel length of 3 μm. The a-Si spacer thickness is 2000Å.

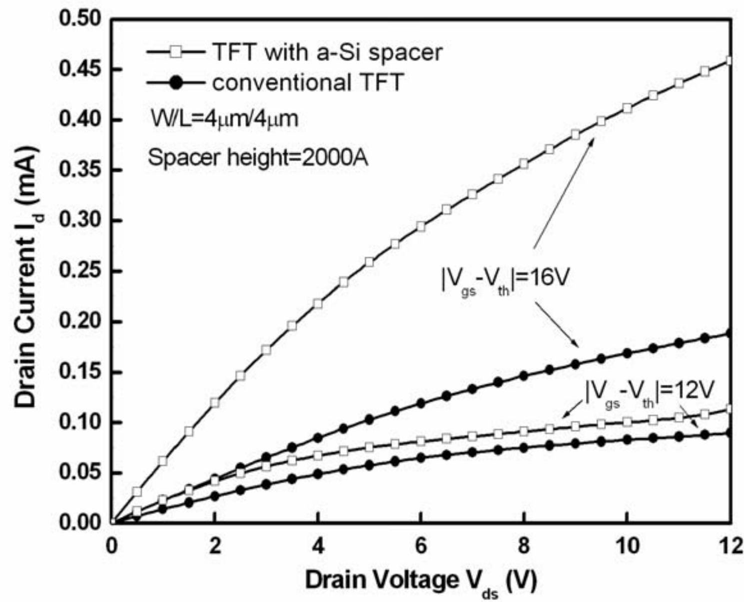

Figure 5.21(d). The output characteristic of poly-Si TFTs crystallized using a-Si spacer structure with channel length of 4 μm. The a-Si spacer thickness is 2000Å.

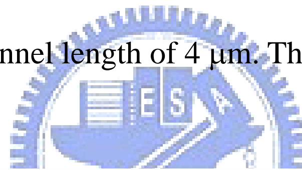

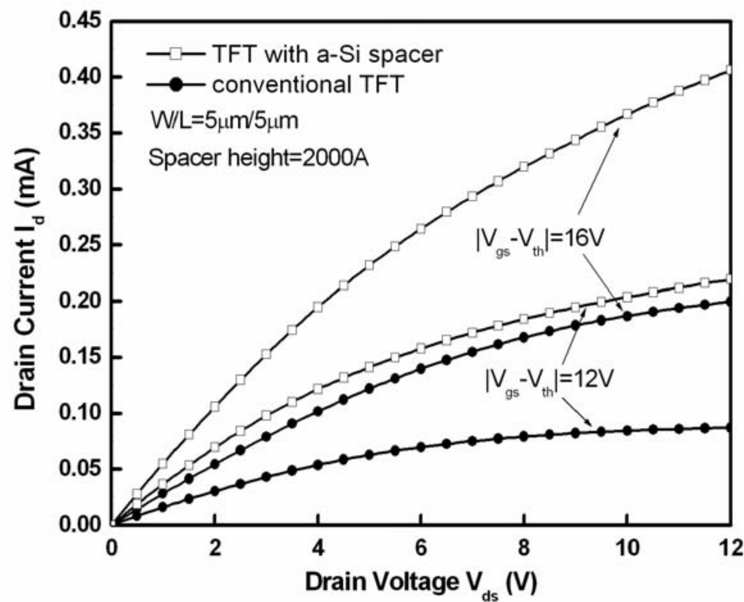

Figure 5.21(e). The output characteristic of poly-Si TFTs crystallized using a-Si spacer structure with channel length of 5 μm. The a-Si spacer thickness is 2000Å.